Nanoscale

RSC Publishing

PAPER

View Article Online
View Journal | View Issue

Published on 03 June 2013. Downloaded by University of California - Santa Cruz on 26/07/2013 01:10:52.

Trimetallic Ag@AuPt Neapolitan nanoparticles

Cite this: *Nanoscale*, 2013, **5**, 7284

Yang Song and Shaowei Chen*

Trimetallic Ag@AuPt Neapolitan nanoparticles were prepared by two sequential galvanic exchange reactions of 1-hexanethiolate-capped silver nanoparticles (AgC6, 5.70 ± 0.82 nm in diameter) with gold(I)-thiomalic acid (Au^{I}TMA) and platinum(II)-hexanethiolate (Pt^{II}C6) complexes. The first reaction was carried out at the air–water interface by the Langmuir method where the AgC6 nanoparticles formed a compact monolayer and water-soluble Au^{I}TMA was injected into the water subphase; the nanoparticles were then deposited onto a substrate surface in the up-stroke fashion and immersed into an acetone solution of Pt^{II}C6. As both reactions were confined to an interface, the Au and Pt elements were situated on two opposite poles of the original Ag nanoparticles. The tripatchy structure was clearly manifested in elemental mapping of the nanoparticles, and consistent with the damping and red-shift of the nanoparticle surface plasmon resonance. Further characterizations by X-ray photoelectron spectroscopy showed that the reactions were mostly confined to the top layers of the Ag metal cores, and contact angle and infrared spectroscopic measurements confirmed the incorporation and segregated distribution of the organic capping ligands on the nanoparticle surface.

Received 3rd May 2013
Accepted 31st May 2013

DOI: 10.1039/c3nr02269b

www.rsc.org/nanoscale

Introduction

As unique structural scaffolds, nanoparticles may be decorated with multiple functional moieties. Yet, in most prior research these functional moieties are distributed rather homogeneously on the nanoparticle surface. To further engineer the nanoparticle structures and manipulate the properties and functions, there has been a great deal of interest in the design and preparation of patchy nanoparticles with an asymmetrical distribution of the organic and/or metal components within the nanoparticles. Such directional engineering of the nanoparticles may then be exploited for an unprecedented control of the self-assembled nanoparticle structures.[1–4] Towards this end, amphiphilic Janus nanoparticles have represented the first example of bi-patchy nanoparticles that exhibit two hemispheres of distinctly different chemical compositions and/or properties.[1] Yet, is it possible to have more complicated chemical patterning of the nanoparticles with a multi-patchy surface structure? This is the primary motivation of the present study.

It should be noted that experimental preparation of such multipatchy particles has been mostly focused on (sub)micron-sized polymeric particles that are produced by, for instance, particle and nanosphere lithography, and glancing-angle deposition.[5] In these, the self-assembly of block copolymers has been suggested as an effective route for the fabrication of functional patchy particles, where the composition and distribution of the solvophilic and solvophobic components are proposed to play a critical role in the manipulation of the interparticle interactions and hence organized assemblies.[6]

In contrast, the study of nanometer-sized metal particles with patchy metal compositions and/or organic capping layers is largely limited to theoretical simulations and modeling. For instance, Pons-Siepermann and Glotzer[7] carried out computer simulations based on dissipative particle dynamics (DPD) to predict the patterns of a mixed monolayer consisting of three thiol derivatives self-assembled on gold nanoparticle surfaces. With a deliberate variation of four critical parameters: (a) nanoparticle core diameter, (b) degree of ligand immiscibility, (c) ligand chain length, and (d) monolayer composition, they predicted the formation of various patchy structures, including striped Janus particles, tri-patchy Neapolitan and Cerberus nanoparticles, *etc.*

It should be emphasized that whereas there has been much progress in theoretical simulations and modelling, experimental preparation of such multi-patchy nanoparticles has remained a great challenge. In the present study, we took advantage of our prior progress in the preparation of Janus nanoparticles with asymmetric organic capping patches,[8–10] and demonstrated that trimetallic Ag@AuPt Neapolitan nanoparticles might be readily prepared by interfacial engineering based on the Langmuir methods and galvanic replacement reactions. The procedure is depicted in Scheme 1. Specifically, 1-hexanethiolate-passivated silver (AgC6) nanoparticles were used as the starting materials. A compact monolayer was formed on the water surface of a Langmuir–Blodgett tough, into which a calculated amount of gold(I)-thiomalic acid (Au^{I}TMA) complex was injected. Galvanic exchange reactions between the AgC6 nanoparticles and Au^{I}TMA at the air–water interface led to the displacement of part of the Ag atoms on the bottom side of the nanoparticle cores with Au and

Department of Chemistry and Biochemistry, University of California, 1156 High Street, Santa Cruz, California 95064, USA. E-mail: Shaowei@ucsc.edu

This journal is © The Royal Society of Chemistry 2013

Published on 03 June 2013. Downloaded by University of California - Santa Cruz on 26/07/2013 01:10:52.

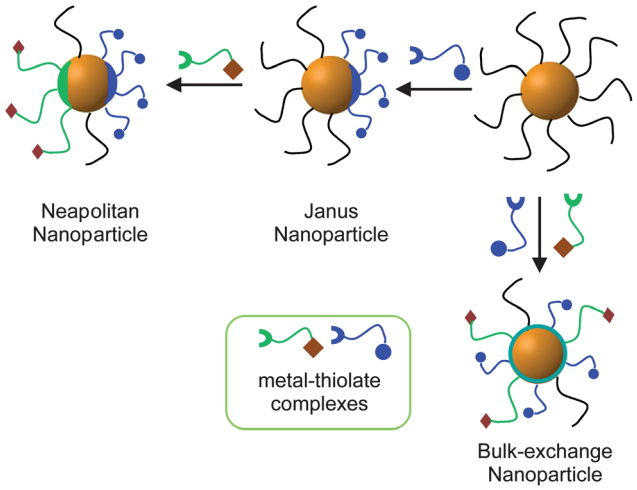

Scheme 1 Preparation of trimetallic Neapolitan and bulk-exchange nanoparticles by interfacial galvanic exchange reactions.

concurrently the replacement of the original hydrophobic hexanethiolate ligands with the more hydrophilic TMA ones. The monolayer was then up-stroke deposited onto a glass slide surface by the Langmuir–Blodgett method (such that the hexanethiolate side was exposed), and immersed into a solution of platinum(II)-hexanethiolate ($Pt^{II}C6$) complex for the second galvanic replacement reactions. As both reactions were restricted to two opposite sides of the nanoparticles, the resulting particles exhibited a segregated distribution of three metal components (Ag, Au and Pt) as well as organic capping ligands. To the best of our knowledge, we believe that this is the first experimental demonstration of nanometer-sized trimetallic Neapolitan particles. As a control experiment, trimetallic Ag@AuPt nanoparticles were also prepared by galvanic exchange reactions of AgC6 nanoparticles with $Au^{I}TMA$ and $Pt^{II}C6$ in THF. The resulting nanoparticles were denoted as bulk-exchange nanoparticles.

Experimental section

Chemicals

Hydrogen tetrachloroauric acid ($HAuCl_4 \cdot xH_2O$) was synthesized by dissolving ultrahigh-purity gold (99.999%, Johnson Matthey) in freshly prepared aqua regia followed by crystallization.[11] Silver nitrate ($AgNO_3$, Fisher Scientific), platinum chloride ($PtCl_2$, ACROS), sodium borohydride ($NaBH_4$, ≥98%, ACROS), tetra-*n*-octylammonium bromide (TOABr, 98%, ACROS), 1-hexanethiol (C6SH, 96%, ACROS), and thiomalic acid (TMA, Aldrich, 95%) were all used as received without any further purification. Solvents were purchased at the highest purity available from typical commercial sources and also used as received. Water was supplied by a Barnstead Nanopure water system (18.3 MΩ cm).

The $Au^{I}TMA$ complex was prepared by mixing a stoichiometric amount of $HAuCl_4$ and TMA in acetone, which was a light yellow precipitate as a result of the reduction of Au^{III} to Au^{I} by the thiol moiety.[12] The precipitate was collected by centrifugation and washed extensively with acetone and finally dissolved in water at a concentration of 1 mM. The $Pt^{II}C6$ complex was prepared by mixing a $PtCl_2$ aqueous solution with hexanethiol in chloroform. The formation of $Pt^{II}C6$ was signified by the colour appearance in the chloroform phase whereas the water phase became colourless. The chloroform phase was collected, dried and further washed with methanol to remove excessive thiols, affording $Pt^{II}C6$ that was soluble in acetone.

Synthesis of silver nanoparticles

1-Hexanethiolate-passivated silver (AgC6) nanoparticles were prepared by following the Brust method.[13] Experimentally, 30 mL of an aqueous $AgNO_3$ solution (0.03 M) was mixed with 20 mL of a toluene solution of TOABr (0.20 M) and stirred vigorously for 1 h. The grey organic phase was collected, into which 150 μL of 1-hexanethiol was added with a Hamilton microliter syringe. After the solution was stirred for 15 min, 24 mL of a freshly prepared ice-cold aqueous solution of 0.43 M $NaBH_4$ was added dropwise, and the solution colour turned dark brown immediately, signifying the formation of silver nanoparticles. The reaction mixture was stirred for 4 h before the organic phase was collected and washed five times with methanol to remove the phase-transfer catalysts, excessive 1-hexanethiol, and reaction by-products. The resulting silver nanoparticles were denoted as AgC6.

Preparation of trimetallic Neapolitan nanoparticles

The trimetallic Neapolitan nanoparticles were prepared by two-step interfacial galvanic replacement reactions of AgC6 nanoparticles with $Au^{I}TMA$ and $Pt^{II}C6$ complexes. The first step was similar to that used to prepare bimetallic AgAu Janus nanoparticles that was detailed previously.[10] In brief, a monolayer of AgC6 nanoparticles was deposited onto the water surface of a Langmuir–Blodgett trough (NIMA Technology, model 611D). The particle monolayer was then compressed to a desired surface pressure where the interparticle edge-to-edge separation was maintained at a value smaller than twice the extended ligand chain length such that the interfacial mobility of the particles was impeded. At this point, a calculated amount of the $Au^{I}TMA$ aqueous solution was injected into the water subphase by a Hamilton microliter syringe, where the first interfacial galvanic exchange reactions occurred leading to the formation of AgC6–AuTMA bimetallic Janus nanoparticles.[10] The nanoparticle monolayers were then transferred onto a clean glass slide surface (8 cm × 3 cm) by the up-stroke deposition method so that the hydrophobic side with the hexanethiolate ligands was exposed. Then the glass slides were immersed into an acetone solution of the $Pt^{II}C6$ complex for the second interfacial galvanic replacement reaction (this procedure was used previously in the preparation of another type of Janus nanoparticles[9]), which took place at the hexanethiolate face of the particles that was in direct contact with the acetone solution, resulting in the generation of trimetallic Neapolitan nanoparticles (Scheme 1). Then, the glass slides with Neapolitan nanoparticle monolayers were gently rinsed with copious amounts of acetone and dried in a gentle stream of ultrahigh-purity nitrogen before being collected into a glass vial by THF. At least four batches of particle samples were prepared and

Published on 03 June 2013. Downloaded by University of California - Santa Cruz on 26/07/2013 01:10:52.

collected under identical conditions so that there were enough materials for further analyses. The resulting Neapolitan particles were found to be soluble in chloroform and THF.

As a control measurement, galvanic replacement reactions of the AgC6 nanoparticles with $Au^{I}TMA$ and $Pt^{II}C6$ complexes were also carried out by mixing a calculated amount of AgC6 nanoparticles with $Au^{I}TMA$ and $Pt^{II}C6$ complexes in THF under magnetic stirring for 8 h. The solution was then dried under reduced pressure with a rotary evaporator, and excessive ligands were removed by extensive rinsing with methanol. The resulting particles were denoted as bulk-exchange particles and, similar to the Neapolitan nanoparticles, were soluble in chloroform and THF.

Characterizations

Contact angles were measured with a Tantec CAM-PLUS contact angle meter. For each sample, at least ten independent measurements were carried out for statistical analyses. The UV-vis spectra were collected with a UNICAM ATI UV4 spectrometer at a particle concentration of *ca.* 0.5 mg mL^{-1} in THF using a 1 cm quartz cuvette. X-ray photoelectron (XPS) spectra were recorded with a PHI 5400/XPS instrument equipped with an Al Kα source operated at 350 W and 10^{-9} Torr. Silicon wafers were sputtered by argon ions to remove carbon from the background and used as substrates. The morphology and sizes of the nanoparticles were characterized by transmission electron microscopic studies (TEM, Philips CM200 at 200 kV). At least 200 nanoparticles were measured to obtain a size histogram. Energy-dispersive X-ray spectroscopy (EDS) studies were carried out by using a Philips CM200/FEG transmission electron microscope.

Results and discussion

The structures of the resulting nanoparticles were first examined by transmission electron microscopic (TEM) measurements. Fig. 1 depicts the representative TEM micrographs of the (A) original AgC6, (B) trimetallic Ag@AuPt bulk-exchange and (C) Neapolitan nanoparticles. It can be seen that the nanoparticles were all very well dispersed, indicating effective protection of the nanoparticles by the thiolate ligands before and after core metal galvanic exchange reactions. Also, the nanoparticle core size remained statistically unchanged. In fact, the average core diameter was found to be 5.70 $\pm$ 0.82 nm, 6.00 $\pm$ 0.75 nm, and 5.90 $\pm$ 0.76 nm for the as-prepared AgC6, trimetallic bulk-exchange, and Neapolitan particles, respectively (right insets). Furthermore, the nanoparticles all exhibited well-defined crystalline lattice fringes, with a spacing of 0.23 nm, as highlighted in the left insets. This is consistent with the Ag(111) crystal planes,[14] and implies that only a small fraction of the Ag atoms on the original nanoparticle surface was replaced by Au and Pt, in agreement with XPS measurements (*vide infra*).

The tri-patchy characteristics of the Neapolitan nanoparticles were then manifested in EDS elemental mapping. Fig. 2 shows two representative elemental maps of (A) trimetallic bulk-exchange and (B) Neapolitan nanoparticles with the red symbols for silver, green for gold and blue for platinum. It can be seen that for the bulk-exchange nanoparticles in panel (A) the three metal

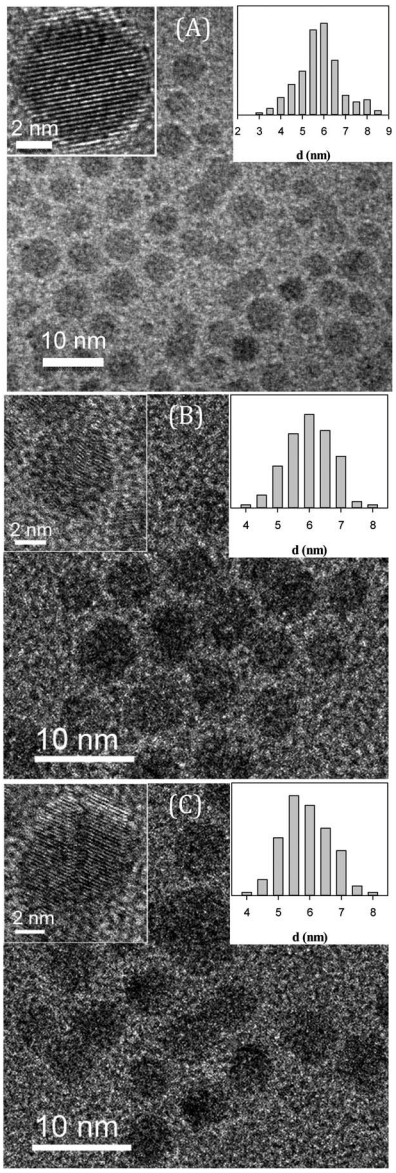

Fig. 1 Representative TEM images of (A) AgC6 nanoparticles, (B) trimetallic Ag@AuPt bulk-exchange and (C) Neapolitan nanoparticles. The scale bars are all 10 nm. Left insets show the corresponding high-resolution TEM micrographs with the scale bars of 2 nm. Right insets are the respective core size histograms.

elements were distributed rather homogeneously throughout the entire nanoparticles. By contrast, for the Neapolitan nanoparticles in panel (B), whereas the silver signals can be identified all over the nanoparticles, the gold and platinum elements are clearly segregated on two opposite poles of the nanoparticles, as highlighted in the schematic of panel (C).

The replacement of part of the Ag atoms on the nanoparticle surface by Au and Pt led to an apparent variation of the nanoparticle optical properties. Fig. 3 depicts the UV-vis absorption spectra of the AgC6, and trimetallic Ag@AuPt bulk-exchange and Neapolitan nanoparticles in THF. For the original AgC6 nanoparticles (solid curve), the surface plasmon resonance peak can be clearly identified at 419 nm.[15] Yet for the trimetallic bulk-exchange (dotted curve) and Neapolitan (dashed curve) nanoparticles, the peak became broadened somewhat and

 This journal is © The Royal Society of Chemistry 2013

Published on 03 June 2013. Downloaded by University of California - Santa Cruz on 26/07/2013 01:10:52.

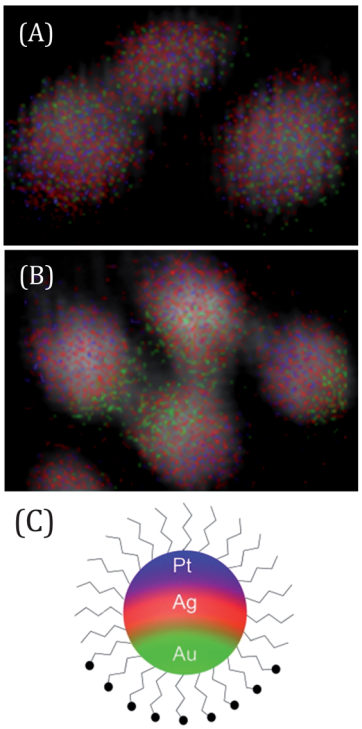

Fig. 2 Representative false-colour EDS elemental maps of (A) bulk-exchange and (B) Neapolitan nanoparticles with red symbols for Ag, green for Au and blue for Pt. The samples are the same as those as in Fig. 1(B) and (C). Panel (C) is a schematic of the resulting Neapolitan nanoparticles.

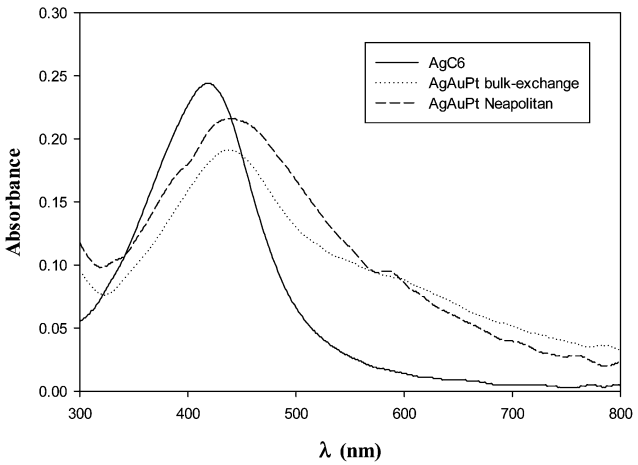

Fig. 3 UV-vis spectra of AgC6 nanoparticles (solid curve), trimetallic bulk-exchange (dotted curve) and Neapolitan (dashed curve) nanoparticles in THF at a concentration of about 0.5 mg mL^{-1}.

red-shifted to 437 nm, along with the emergence of a broad shoulder centered at around 589 nm. The first peak most likely arose from the damping of the Ag surface plasmon by the Au(Pt) overlayer, whereas the second peak might be ascribed to the deposition of Au (Pt) onto the Ag nanoparticle surface in the form of tiny clusters where alloying occurred at the bimetallic interface. Similar observations were reported with much larger Ag@AgAu metal core–alloy shell nanoparticles (*ca.* 18 nm in diameter) that were prepared also by galvanic exchange reactions, which were accounted for by the plasmon hybridization theory.[16] In addition, unlike Ag and Au nanoparticles, Pt nanoparticles exhibit no well-defined surface plasmon resonance.[15] Therefore, in the trimetallic Ag@AuPt nanoparticles the optical features were largely determined by the Ag and Au components. In fact, one may notice that such optical characteristics were also observed previously with bimetallic AgAu Janus and bulk-exchange nanoparticles prepared with the same AgC6 nanoparticles (Scheme 1),[10,17] as well as Au@Ag and Ag@Au core–shell nanoparticles.[18–20]

The incorporation of Au and Pt onto the Ag nanoparticles by galvanic exchange reactions was also manifested in XPS measurements. Fig. 4 shows the XPS survey spectra of (A) Ag 3d, (B) Au 4f, and (C) Pt 4f electrons for the Neapolitan (bottom spectra) and bulk-exchange (top spectra) nanoparticles. By deconvolution fits, the Ag 3d electrons can be readily identified at 368.1 and 374.2 eV for the bulk-exchange nanoparticles, and for the Neapolitan counterparts, they are almost unchanged at 368.2 and 374.2 eV. Meanwhile, a rather apparent variation was observed for the Au 4f electrons, which appeared at 83.7 and 87.5 eV for the bulk-exchange nanoparticles and red-shifted to 83.3 and 87.2 eV for the Neapolitan nanoparticles. In contrast, the binding energies of the Pt 4f electrons increased from 71.4 and 74.7 eV for the bulk-exchange nanoparticles to 71.8 and 75.2 eV for the Neapolitan nanoparticles. Overall, these values are comparable to those reported previously for AgAu, AgPt, or AuPt bimetallic core–shell or alloy nanoparticles.[10,21–23] Yet, the apparent discrepancy of the Au 4f and Pt 4f binding energies between the bulk-exchange and Neapolitan nanoparticles seem to suggest that in comparison with the structurally symmetric bulk-exchange nanoparticles, the segregation of Au and Pt on two opposite poles of the Neapolitan nanoparticles led to an uneven distribution of electrons where partial charge transfer likely occurred from Pt to Au (the segregated distribution of the associated polar TMA ligands from the apolar hexanethiolates in the Neapolitan nanoparticles and hence the formation of an apparent dipole might also help stabilize the extra electron density on the gold sites[10]). This may be accounted for by the difference of electronegativity of the three metal elements, Au (2.4) > Pt (2.2) > Ag (1.9).[24]

Furthermore, based on the integrated peak areas, the atomic ratio of the metal elements can be estimated to be 1 : 1.6 : 5.6 for the bulk-exchange nanoparticles and 1 : 2.0 : 8.6 for the Neapolitan nanoparticles. That is, the fractions of the Ag core atoms that were replaced by Au and Pt combined was 31.7% and 25.9% for the bulk-exchange and Neapolitan nanoparticles, respectively. Note that based on the average core diameter of the nanoparticles as measured by TEM measurements (Fig. 1), the surface atoms constituted about 25% of the total atoms of the metal cores of these nanoparticles.[25] This means that in the preparation of the bulk-exchange and Neapolitan nanoparticles, the galvanic exchange reactions were mostly limited to the top layers of the Ag cores. Also as the Au/Pt ratio is very close, these two nanoparticles may be approximated as structural isomers.

With regard to the organic capping layer, the first galvanic exchange reactions would incorporate TMA ligands onto the nanoparticle surface, whereas in the second step, the organic

Published on 03 June 2013. Downloaded by University of California - Santa Cruz on 26/07/2013 01:10:52.

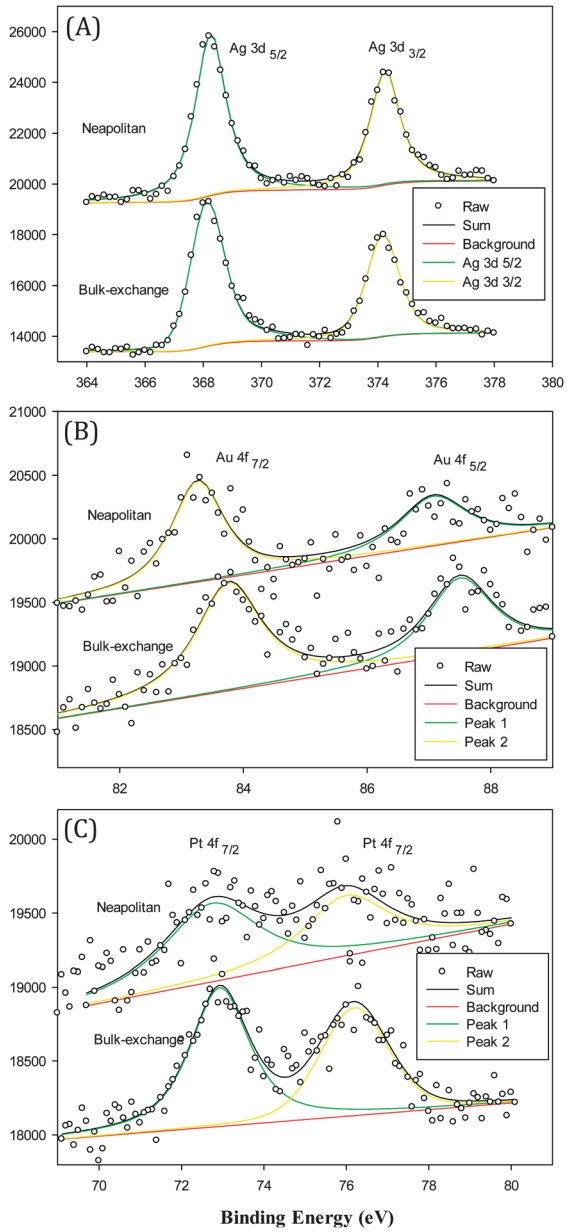

Fig. 4 XPS survey spectra of (A) Ag 3d, (B) Au 4f and (C) Pt 4f electrons in trimetallic Ag@AuPt bulk-exchange (bottom curves) and Neapolitan (top curves) nanoparticles. Symbols are experimental data and lines are deconvolution fits. Data are summarized in Table 1.

ligands remained unchanged (with $Pt^{II}C6$). Thus, the resulting Neapolitan nanoparticles are anticipated to exhibit a surface structure analogous to that of Janus nanoparticles.[8–10] To confirm the amphiphilic characters of the surface protecting layers, a monolayer of nanoparticles was formed at the air–water interface and transferred onto a microscope glass slide by up- and down-stroke deposition, and the thin-film contact angles were measured. For the original AgC6 nanoparticles a consistent contact angle of 94.8 ± 5.1° was observed for both up- and down-stroke depositions, which is consistent with those observed with self-assembled monolayers of alkanethiols on silver substrate surfaces.[26,27] In comparison, the Neapolitan nanoparticles showed a contact angle of 92.8 ± 5.6° when the nanoparticle film was deposited in the up-stroke fashion (that is, with the hydrophobic face of the hexanethiolate ligands exposed), which is similar to that of AgC6 nanoparticles; however, the contact angle exhibited a marked diminishment to 30.8 ± 4.1° when the nanoparticle monolayers were deposited by the down-stroke method (with the hydrophilic side of the TMA ligands exposed). Note that the latter is consistent with that observed with a TMA self-assembled monolayer on Au thin film surfaces (27.4 ± 7.2°). These observations suggest the effective replacement of the original hydrophobic hexanethiolate ligands by the more hydrophilic TMA during galvanic exchange reactions, and the TMA and C6 ligands were segregated on the nanoparticle surface. Similar behaviours have been observed previously in galvanic exchange reactions of AgC6 nanoparticles with gold(I)-mercaptopropanediol ($Au^{I}MPD$) complex,[10] and ligand exchange reactions of AuC6 nanoparticles with 2-(2-mercaptoethoxy)-ethanol (MEA)[9] and 3,5-octadiyne-1-ol-8-thiol (DAT)[28] as the hydrophilic ligands.

The incorporation of the TMA ligands into the nanoparticle surface capping layer is further manifested in FTIR measurements. Fig. 5 depicts the FTIR spectra of the original AgC6 nanoparticles, trimetallic Ag@AuPt bulk-exchange and Neapolitan nanoparticles, as well as the $Au^{I}TMA$ and $Pt^{II}C6$ complexes. In comparison with the spectral data of the AgC6 nanoparticles (black curve), bulk-exchange (red curve) and Neapolitan nanoparticles (green curve) share the same vibrational features that are consistent with the vibrational characteristics of the 1-hexanethiolate ligands (which can also be observed with the $Pt^{II}C6$ complex, yellow curve), including the methyl and methylene C–H stretches between 2800 and 3000 cm^{-1}, methylene C–H rocking at 1463 cm^{-1} and methyl C–H bending at 1377 cm^{-1}.[29] Meanwhile, several new features emerged for the bulk-exchange (red curve) and Neapolitan nanoparticles (green curve), including the O–H stretch at 3450 cm^{-1} and carboxylic C=O stretch at 1710 cm^{-1} (the peak at 1592 cm^{-1} suggests the presence of carboxylate anions in the TMA ligands) which are consistent with the vibrational characteristics of the $Au^{I}TMA$ complex (blue curve). Note that the vibrational stretch of S–H (~2550 cm^{-1}) was not observed in any

Table 1 Binding energies of the Ag 3d, Au 4f and Pt 4f electrons in trimetallic Ag@AuPt bulk-exchange and Neapolitan nanoparticles and the Au/Ag/Pt atomic ratios by XPS measurements

	Ag		Au		Pt		
	$3d_{5/2}$ (eV)	$3d_{3/2}$ (eV)	$4f_{7/2}$ (eV)	$4f_{5/2}$ (eV)	$4f_{7/2}$ (eV)	$4f_{5/2}$ (eV)	Au/Pt/Ag atomic ratio
Bulk-exchange	368.1	374.2	83.7	87.5	71.4	74.7	1 : 1.6 : 5.6
Neapolitan	368.2	374.2	83.3	87.2	71.8	75.2	1 : 2.0 : 8.6

This journal is © The Royal Society of Chemistry 2013

Published on 03 June 2013. Downloaded by University of California - Santa Cruz on 26/07/2013 01:10:52.

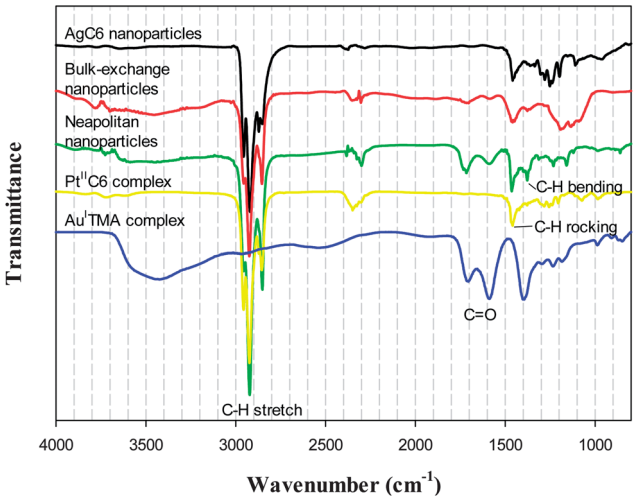

Fig. 5 FTIR spectra of the AgC6 nanoparticles (black curve), trimetallic Ag@AuPt bulk-exchange (red curve) and Neapolitan (green curve) nanoparticles, along with the Au^{I}TMA (yellow curve) and Pt^{II}C6 (blue curve) complexes.

of the samples, indicating that the samples were free of excessive thiol ligands.

Conclusion

In this study a Langmuir-based interfacial engineering approach was developed for the first-ever preparation of trimetallic Neapolitan nanoparticles. Using 1-hexanethiolate-protected Ag nanoparticles as the starting materials, Ag@AuPt Neapolitan nanoparticles were prepared by two sequential galvanic exchange reactions with Au(I)-thiomalic acid and platinum(II)-hexanethiolate complexes. As these two reactions were confined on two opposite sides of the Ag nanoparticles, there was a clear segregation of the Au and Pt elements (and the corresponding organic capping ligands) on the nanoparticle surface, as manifested in EDS elemental mapping studies as well as spectroscopic measurements. Such an unprecedented level of engineering of the nanoparticle structures may pave the way towards increasingly deliberate manipulation of the nanoparticle properties and functions. This is being pursued in ongoing work and results will be reported in due course.

Acknowledgements

This work was supported in part by the National Science Foundation (DMR-0804049, CHE-1012256 and CBET-1258839). TEM and XPS studies were carried out at the National Center for Electron Microscopy and the Molecular Foundry, Lawrence Berkeley National Laboratory, as part of a user project.

Notes and references

1 Z. L. Zhang and S. C. Glotzer, *Nano Lett.*, 2004, **4**, 1407–1413.
2 S. Jiang, Q. Chen, M. Tripathy, E. Luijten, K. S. Schweizer and S. Granick, *Adv. Mater.*, 2010, **22**, 1060–1071.
3 Q. Chen, S. C. Bae and S. Granick, *Nature*, 2011, **469**, 381–384.
4 Q. Chen, J. K. Whitmer, S. Jiang, S. C. Bae, E. Luijten and S. Granick, *Science*, 2011, **331**, 199–202.
5 A. B. Pawar and I. Kretzschmar, *Macromol. Rapid Commun.*, 2010, **31**, 150–168.
6 J. Zhang, Z. Y. Lu and Z. Y. Sun, *Soft Matter*, 2011, **7**, 9944–9950.
7 I. C. Pons-Siepermann and S. C. Glotzer, *Soft Matter*, 2012, **8**, 6226–6231.
8 S. Pradhan, L. P. Xu and S. W. Chen, *Adv. Funct. Mater.*, 2007, **17**, 2385–2392.
9 S. Pradhan, L. E. Brown, J. P. Konopelski and S. W. Chen, *J. Nanopart. Res.*, 2009, **11**, 1895–1903.
10 Y. Song, K. Liu and S. Chen, *Langmuir*, 2012, **28**, 17143–17152.
11 G. Brauer, *Handbook of preparative inorganic chemistry*, Academic Press, New York, 1963.
12 K. Nomiya, K. I. Onoue, Y. Kondoh, N. C. Kasuga, H. Nagano, M. Oda and S. Sakuma, *Polyhedron*, 1995, **14**, 1359–1367.
13 M. Brust, M. Walker, D. Bethell, D. J. Schiffrin and R. Whyman, *J. Chem. Soc., Chem. Commun.*, 1994, 801–802.
14 J. Q. Tian, S. Liu, Y. W. Zhang, H. Y. Li, L. Wang, Y. L. Luo, A. M. Asiri, A. O. Al-Youbi and X. P. Sun, *Inorg. Chem.*, 2012, **51**, 4742–4746.
15 J. A. Creighton and D. G. Eadon, *J. Chem. Soc., Faraday Trans.*, 1991, **87**, 3881–3891.
16 Q. B. Zhang, J. P. Xie, J. Y. Lee, J. X. Zhang and C. Boothroyd, *Small*, 2008, **4**, 1067–1071.
17 Y.-S. Shon, G. B. Dawson, M. Porter and R. W. Murray, *Langmuir*, 2002, **18**, 3880–3885.
18 P. Mulvaney, M. Giersig and A. Henglein, *J. Phys. Chem.*, 1993, **97**, 7061–7064.
19 Y. S. Shon, G. B. Dawson, M. Porter and R. W. Murray, *Langmuir*, 2002, **18**, 3880–3885.
20 S. Pande, S. K. Ghosh, S. Praharaj, S. Panigrahi, S. Basu, S. Jana, A. Pal, T. Tsukuda and T. Pal, *J. Phys. Chem. C*, 2007, **111**, 10806–10813.
21 S. P. Mulvaney, M. D. Musick, C. D. Keating and M. J. Natan, *Langmuir*, 2003, **19**, 4784–4790.
22 M. A. Uppal, M. B. Ewing and I. P. Parkin, *Eur. J. Inorg. Chem.*, 2011, **2011**, 4534–4544.
23 C. Xu, R. Wang, M. Chen, Y. Zhang and Y. Ding, *Phys. Chem. Chem. Phys.*, 2010, **12**, 239–246.
24 D. R. Lide, *CRC Handbook of Chemistry and Physics*, CRC Press, Boca Raton, FL, 2001.
25 M. J. Hostetler, J. E. Wingate, C. J. Zhong, J. E. Harris, R. W. Vachet, M. R. Clark, J. D. Londono, S. J. Green, J. J. Stokes, G. D. Wignall, G. L. Glish, M. D. Porter, N. D. Evans and R. W. Murray, *Langmuir*, 1998, **14**, 17–30.
26 P. E. Laibinis, M. A. Fox, J. P. Folkers and G. M. Whitesides, *Langmuir*, 1991, **7**, 3167–3173.
27 Y. T. Tao and M. T. Lee, *Thin Solid Films*, 1994, **244**, 810–814.
28 Y. Song, L. M. Klivansky, Y. Liu and S. W. Chen, *Langmuir*, 2011, **27**, 14581–14588.
29 R. M. Silverstein, F. X. Webster and D. J. Kiemle, *Spectrometric identification of organic compounds*, John Wiley & Sons, Hoboken, NJ, 2005.